Received: 27 September 2021 | Revised: 24 November 2021 | Accepted: 29 November 2021

DOI: 10.1111/mpp.13175

Molecular Plant Pathology WILEY

ORIGINAL ARTICLE

An unconventionally secreted effector from the root knot nematode *Meloidogyne incognita*, Mi-ISC-1, promotes parasitism by disrupting salicylic acid biosynthesis in host plants

Xin Qin[1,2] | Bowen Xue[1,2] | Haiyang Tian[1,2] | Chenjie Fang[1,2] | Jiarong Yu[1,2] | Cong Chen[1,2] | Qing Xue[1,2] | John Jones[3,4] | Xuan Wang[1,2]

[1]Key Laboratory of Integrated Management of Crop Disease and Pests, Ministry of Education, Nanjing Agricultural University, Nanjing, China

[2]Key Laboratory of Plant Immunity, Nanjing Agricultural University, Nanjing, China

[3]School of Biology, Biomedical Sciences Research Complex, University of St Andrews, St Andrews, UK

[4]Cell & Molecular Sciences Department, The James Hutton Institute, Dundee, UK

Correspondence
Xuan Wang, Key Laboratory of Integrated Management of Crop Disease and Pests, Ministry of Education, Nanjing Agricultural University, Nanjing 210095, China.
Email: xuanwang@njau.edu.cn

Funding information
National Natural Science Foundation of China, Grant/Award Number: 31872923 and 31371922; Scottish Government Rural and Environmental Science and Analytical Services Division

Abstract

Plant-parasitic nematodes need to deliver effectors that suppress host immunity for successful parasitism. We have characterized a novel isochorismatase effector from the root-knot nematode *Meloidogyne incognita*, named Mi-ISC-1. The *Mi-isc-1* gene is expressed in the subventral oesophageal glands and is up-regulated in parasitic-stage juveniles. Tobacco rattle virus-induced gene silencing targeting *Mi-isc-1* attenuated *M. incognita* parasitism. Enzyme activity assays confirmed that Mi-ISC-1 can catalyse hydrolysis of isochorismate into 2,3-dihydro-2,3-dihydroxybenzoate in vitro. Although Mi-ISC-1 lacks a classical signal peptide for secretion at its N-terminus, a yeast invertase secretion assay showed that this protein can be secreted from eukaryotic cells. However, the subcellular localization and plasmolysis assay revealed that the unconventional secretory signal present on the Mi-ISC-1 is not recognized by the plant secretory pathway and that the effector was localized within the cytoplasm of plant cells, but not apoplast, when transiently expressed in *Nicotiana benthamiana* leaves by agroinfiltration. Ectopic expression of Mi-ISC-1 in *N. benthamiana* reduced expression of the *PR1* gene and levels of salicylic acid (SA), and promoted infection by *Phytophthora capsici*. The cytoplasmic localization of Mi-ISC-1 is required for its function. Moreover, Mi-ISC-1 suppresses the production of SA following the reconstitution of the de novo SA biosynthesis via the isochorismate pathway in the cytoplasm of *N. benthamiana* leaves. These results demonstrate that *M. incognita* deploys a functional isochorismatase that suppresses SA-mediated plant defences by disrupting the isochorismate synthase pathway for SA biosynthesis to promote parasitism.

KEYWORDS
effector, isochorismatase, *Meloidogyne incognita*, parasitism, plant immunity, salicylic acid, secretion activity

1 | INTRODUCTION

Root-knot nematodes (*Meloidogyne* spp., RKN) are obligate, sedentary endoparasites that are distributed worldwide. These nematodes can infest more than 3000 plant species, including crops, vegetables, and fruit trees, and the damage to global agriculture is estimated at around $173 billion annually. *Meloidogyne incognita* is the most widely distributed species and is responsible for the largest part of these losses (Elling, 2013; Reddy, 2021).

Plants have evolved a two-layered immune system to withstand pathogen attack, consisting of pathogen-associated molecular pattern (PAMP)-triggered immunity (PTI) and effector-triggered immunity (ETI) (Jones & Dangl, 2006). Adapted pathogens, including nematodes, deploy effectors to suppress plant immune systems to facilitate parasitism. For example, overexpression of an *M. incognita* calreticulin Mi-CRT in *Arabidopsis thaliana* suppressed the expression levels of PTI marker genes and callose deposition triggered by elf18 (Jaouannet et al., 2013). Similarly, plants expressing nematode effectors Mh265, HaGland5, and MiMIF-2 also show reduced flg22-induced callose deposition, which is a hallmark of the PTI response (Gleason et al., 2017; Yang, Pan, et al., 2019b; Zhao et al., 2019). In addition, the *Heterodera avenae* effector Ha18764 and several *Globodera pallida* effectors, including RHA1B and numerous SPRYSEC proteins, suppress ETI triggered by Gpa2/RBP-1 in *Nicotiana benthamiana* (Kud et al., 2019; Mei et al., 2015; Yang, Dai, et al., 2019a).

Salicylic acid (SA) is a critical phytohormone that regulates multiple responses of plants to biotic and abiotic stresses. SA is required for systemic acquired resistance (SAR) as well as PTI and ETI responses (Fu & Dong, 2013; Vlot et al., 2009). The SA pathway is targeted by various pathogen effectors due to its importance in plant immunity. The biotrophic tumour-inducing fungus *Ustilago maydis* encodes an active SA hydroxylase that can degrade SA into catechol, thus halting the activation of plant defences (Djamei et al., 2011). A type III effector of *Pseudomonas syringae*, AvrProB, was found to disrupt NPR1-dependent SA signalling to favour bacterial pathogenicity (Chen, Chen, et al., 2017). The *Arabidopsis* downy mildew pathogen *Hyaloperonospora arabidopsidis* (Hpa) secretes a nuclear-localized effector, HaRxL44, that interacts with Mediator subunit MED19a; this results in a decrease of SA-regulated gene expression but enhances jasmonic acid (JA) and ethylene (ET) signalling to compromise host plant defence against Hpa (Caillaud et al., 2013).

As well reducing SA accumulation and interfering with SA signalling pathways, pathogens may also disrupt SA biosynthesis directly to suppress host defences. It is believed that plants produce SA via two metabolic processes. One is the phenylalanine ammonia-lyase (PAL) pathway in which chorismate mutase (CM) catalyses the conversion of chorismate to prephenate, the precursor for tyrosine and phenylalanine synthesis. PAL subsequently converts phenylalanine to *trans*-cinnamic acid, which is a precursor of SA. The other process is the isochorismate synthase (ICS) pathway, which was widely predicted to exist before the discovery of the isochorismate metabolic pathway within the cytoplasm (Rekhter et al., 2019; Torrens-Spence et al., 2019). In the ICS pathway, chorismate is converted to isochorismate and subsequently to SA by a proposed isochorismate pyruvate lyase (IPL) (Dempsey et al., 2011; Mustafa et al., 2009; Strawn et al., 2007; Wildermuth et al., 2001). *U. maydis* targets the PAL pathway by secreting a chorismate mutase (Cmu1) into the cytoplasm of maize cells. Cmu1 may enhance chorismate export from the plastid to the cytosol, where it is converted to prephenate, thus depleting the precursor of SA biosynthesis in the plastid (Djamei et al., 2011). The filamentous pathogens *Phytophthora sojae* and *Verticillium dahliae* secrete isochorismatases (PsIsc1 and VdIsc1, respectively) that target the ICS pathway of SA biosynthesis, competing with host plants and hydrolysing isochorismate and thus disrupting SA metabolism (Liu et al., 2014).

This competition model has also been reported from plant–nematode interactions. Several RKN species, including *M. incognita*, *Meloidogyne javanica*, *Meloidogyne arenaria*, and *Meloidogyne graminicola*, produce CMs, and one of these from *M. incognita* has been experimentally shown to limit SA biosynthesis and promote nematode parasitism (Huang et al., 2005; Lambert et al., 1999; Long et al., 2006; Wang et al., 2018). More recently, a chorismate mutase (HoCM) and an isochorismatase (HoICM) from the migratory nematode *Hirschmanniella oryzae* were characterized. Both were shown to complement mutant *Escherichia coli* strains lacking these enzymes, while transgenic rice plants expressing those effectors showed reductions in secondary metabolites (Bauters et al., 2020). However, details of the role of isochorismatase from plant-parasitic nematodes were not determined.

In the present study, a novel gene, *Mi-isc-1*, whose deduced amino acid sequence contains a conserved isochorismatase domain, was identified from genome data of the sedentary endoparasitic nematode *M. incognita*. Analysis of temporal and spatial expression patterns as well as tobacco rattle virus (TRV)-mediated gene silencing revealed that *Mi-isc-1* may be important in nematode parasitism. Enzyme activity assays showed that Mi-ISC-1 can catalyse hydrolysis of isochorismate, which is a key precursor of SA biosynthesis, into 2,3-dihydro-2,3-dihydroxybenzoate (DDHB) in vitro. Although the protein encoded by *Mi-isc-1* lacks a predicted signal peptide (SP) for secretion, a yeast secretion trap assay showed that it can be secreted from eukaryotic cells. Transient expression analysis further demonstrated that Mi-ISC-1 was localized within the cytoplasm of plant cells and can compromise the SA-mediated resistance to *Phytophthora capsici* on *N. benthamiana*. Moreover, Mi-ISC-1 suppressed the production of SA following the reconstitution of the de novo SA biosynthesis via the isochorismate pathway in the cytoplasm of *N. benthamiana* leaves. Our results reveal that *M. incognita* uses a functional isochorismatase to promote parasitism by disrupting SA biosynthesis in host plants.

2 | RESULTS

2.1 | *Mi-isc-1* is expressed in the subventral oesophageal gland and is up-regulated during the parasitic stages of *M. incognita*

A sequence, named *Mi-isc-1*, was identified in the *M. incognita* predicted gene set that could encode a protein that includes an isochorismatase domain from Ser14 to Glu161 (PF00857)

(Figures S1 and S2). In situ hybridization was performed to determine the tissue localization of *Mi-isc-1* in *M. incognita*. A clear hybridization signal was observed in the subventral oesophageal gland cells of the nematodes (Figure 1a). As expected, no signal was detected in the negative control when using digoxigenin (DIG)-labelled sense probes (Figure 1b). The expression level of *Mi-isc-1* in different developmental stages of *M. incognita* was also examined using reverse transcription quantitative PCR (RT-qPCR). This showed that the accumulation of *Mi-isc-1* mRNA was relatively low in eggs and the preparasitic J2 stage, and the expression of *Mi-isc-1* increased in the parasitic J2 stage, in which its relative level increased approximately 34.5-fold when compared with that in the eggs. The amount of mRNA reached a maximum in the J3 stage, representing an approximately 89.6-fold increase compared with that in the eggs. Subsequently, the transcript level of *Mi-isc-1* was dramatically reduced in the J4 stage, then in females, decreasing to the same level as that in the pre-J2 stage (Figure 1c). These results suggest that *Mi-isc-1* may play an important role during *M. incognita* parasitism.

2.2 | Silencing of *Mi-isc-1* affects *M. incognita* parasitism

To investigate the role that Mi-ISC-1 plays in the plant–nematode interaction, the expression of *Mi-isc-1* was knocked down during *M. incognita* infection via TRV-mediated RNA interference (Valentine et al., 2007), and the impact of this on nematode parasitism was evaluated. RT-PCR revealed that the transcripts of the TRV coat protein-encoding gene were detected in roots of all TRV lines as early as at 7 days postinfiltration (dpi), suggesting that the TRV particles had already spread to roots and were available for the nematodes to ingest. After this, the viruses continuously replicated in the roots at least for 3 weeks (Figure 2a). The expression level of *Mi-isc-1* was analysed by RT-qPCR at 14 days after nematode inoculation. These experiments showed that the transcripts of *Mi-isc-1* were reduced in nematodes recovered from the TRV::*Mi-isc-1*-infiltrated plants compared with those from the TRV::*gfp*-infiltrated plants or noninfiltrated plants (Figure 2b). Moreover, the average number of galls and egg masses recovered from TRV::*Mi-isc-1* infiltrated plants was significantly reduced, by 16.8% and 27.0%, respectively, when compared with the TRV::*gfp* line. No significant difference was observed either in the *Mi-isc-1* expression or nematode numbers between the TRV::*gfp*-infiltrated plants and the noninfiltrated control plants (Figure 2c). These results suggest that Mi-ISC-1 is essential for the pathogenicity of *M. incognita*.

2.3 | Mi-ISC-1 is a functional isochorismatase that can catalyse the hydrolysis of isochorismate in vitro

Sequence analysis showed that Mi-ISC-1 displayed high similarities to isochorismatases from both prokaryotes and eukaryotes (Figure S3) (Bauters et al., 2020; Caruthers et al., 2005; Drake et al., 2006; Goral et al., 2012; Liu et al., 2012, 2014). To examine whether Mi-ISC-1 is a functional isochorismatase that can hydrolyse isochorismate, as part of the pathway shown in Figure 3a (Drake et al., 2006), we purified the effector protein as well as negative control green fluorescent protein (GFP) following transient expression in *N. benthamiana*. Three key chorismate metabolism enzymes in *E. coli*, EntA, EntB, and EntC, with activities of ICS, isochorismatase, and DDHB dehydrogenase, respectively, were expressed and purified as well, with EntB used as a positive control (Figure 3b). The enzyme activity was determined by observing the increase in absorbance at 340 nm owing to NAD^+ reduction. Both Mi-ISC-1 and EntB exhibited

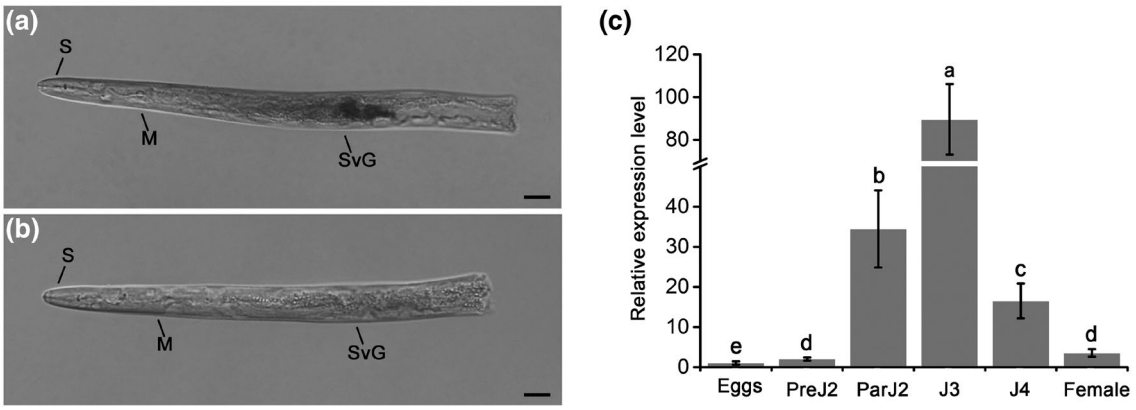

FIGURE 1 Spatial and temporal expression patterns of *Mi-isc-1*. (a) and (b) In situ hybridization showed that the *Mi-isc-1* transcripts were detectable in the subventral oesophageal gland cells of the second-stage juveniles of *Meloidogyne incognita*. The assays were repeated twice with identical results. M, metacorpus; S, stylet; SvG, subventral gland cell. Bar = 10 μm. (c) The transcriptional profiles of *Mi-isc-1* through life stages of *M. incognita*: eggs, preparasitic second-stage juveniles (pre-J2), parasitic J2 (par-J2), third-stage juveniles (J3), fourth-stage juveniles (J4), and female, were quantified using reverse transcription quantitative PCR. The housekeeping gene *actin* was used as a reference. Each column represents the mean relative expression relative to that of the egg. Statistically significant differences using one-way analysis of variance followed by Tukey's test ($p < 0.05$) are indicated with different letters. The results shown are representative of three independent biological experiments

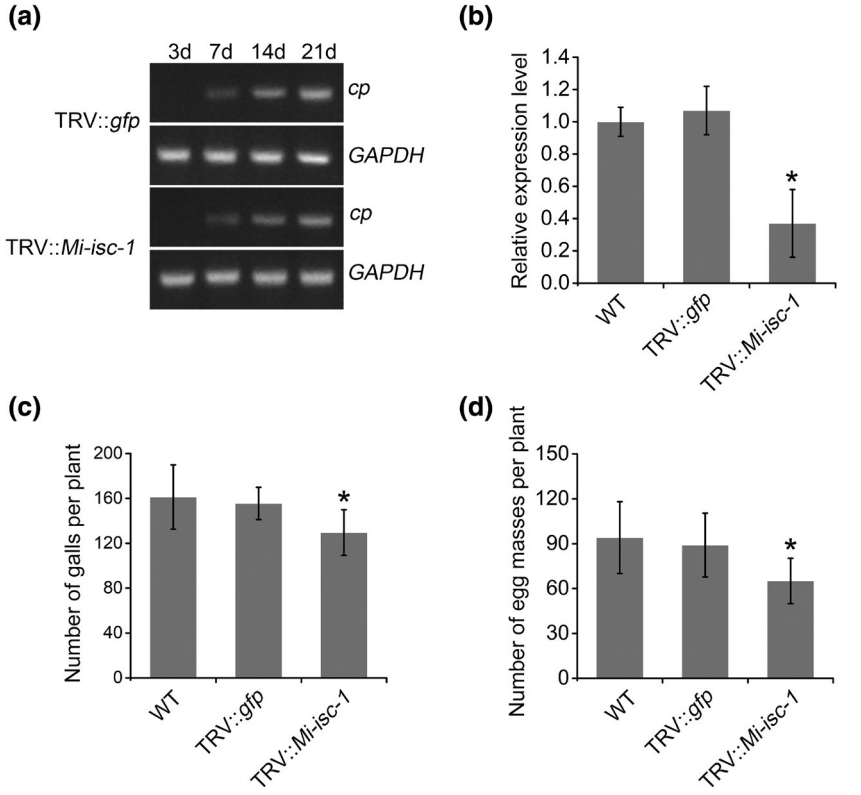

FIGURE 2 In planta RNA interference of *Mi-isc-1* affects *Meloidogyne incognita* parasitism. (a) Reverse transcription PCR detection of the *cp* (coat protein) gene in TRV-infected tomato roots at 3, 7, 14, and 21 days postinoculation (dpi). The *GAPDH* gene of the plant was used as a control. (b) Analysis of the relative expression level of *Mi-isc-1* in *M. incognita* from wild-type (WT) and TRV-infected tomato plants 14 days after nematode inoculation shows that *Mi-isc-1* expression is reduced when grown on plants carrying the silencing construct. (c, d) The number of galls and egg masses produced on different tomato lines at 45 dpi. Data represent the mean and standard deviations obtained from three independent experiments with similar results. Statistically, significant differences were determined using a Student's *t* test (*$p < 0.05$)

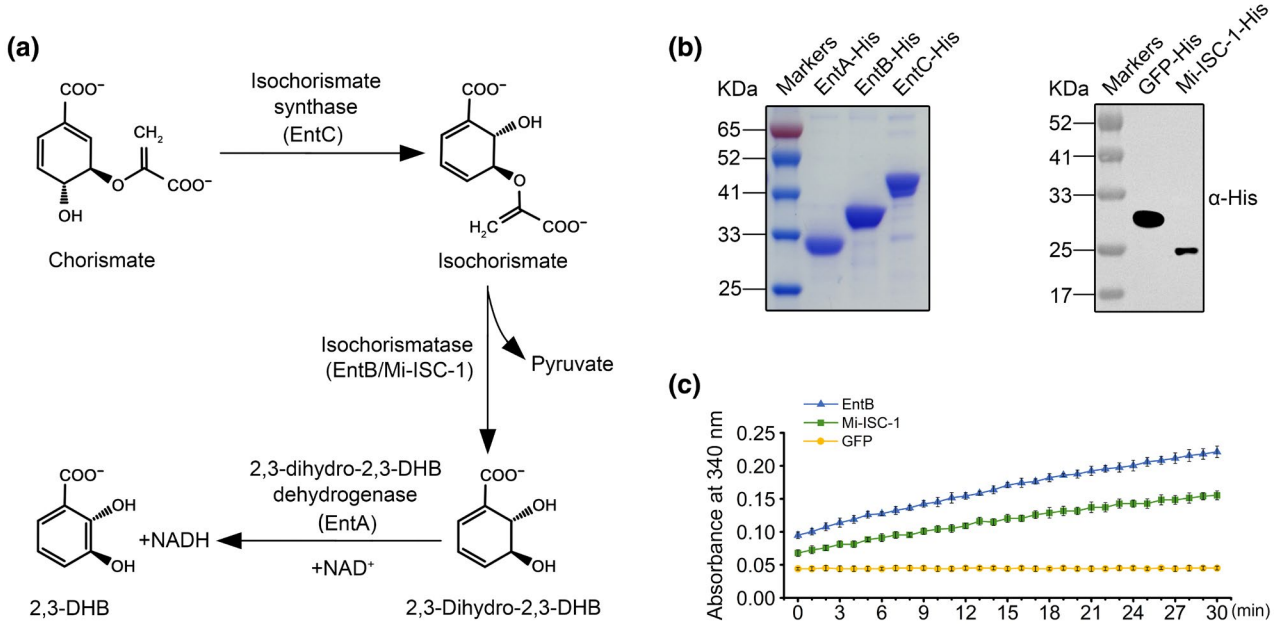

FIGURE 3 Mi-ISC-1 can catalyse the hydrolysis of isochorismate in vitro. (a) The pathway showing the conversion of chorismate to 2,3-dihydroxybenzoate (DHB) via isochorismatase and 2,3-dihydro-2,3-dihydroxybenzoate. (b) The purified recombinant proteins of EntA, EntB, and EntC expressed in *Escherichia coli* BL21 (DE3) were separated by SDS-PAGE (12%) and visualized by Coomassie Brilliant blue G-250 staining. The Mi-ISC-1 and green fluorescent protein (GFP) were purified from *Nicotiana benthamiana* leaves and confirmed by western blot using relevant antibodies. (c) Isochorismatase activity of Mi-ISC-1 was detected by measuring the absorbance of the reaction at 340 nm and was recorded at the indicated time points. The bacterial EntB was used as a positive control and GFP was used as a negative control. The data shown were calculated from three independent biological replicates with similar results

high enzyme activity to convert isochorismate into DDHB, while no signal change was detected when GFP was analysed using the same procedures (Figure 3c). Therefore, the results demonstrate that Mi-ISC-1 has ISC activity.

2.4 | Mi-ISC-1 is an unconventionally secreted protein and its N-terminal is essential for secretion

SignalP analysis showed that the deduced amino acid sequence of Mi-ISC-1 does not contain a predicted N-terminal SP that can direct the protein to the classical secretory pathway (Figure S2). To verify whether Mi-ISC-1 is a secreted protein, we adopted the yeast signal sequence trap assay based on the secretion of invertase for yeast growth on selective media with sucrose or raffinose as the sole carbon source (Jacobs et al., 1997; Oh et al., 2009). The full-length coding sequences of Mi-ISC-1, an N-terminal truncated mutant Mi-ISC-1$^{\Delta N}$, and a C-terminal truncated mutant Mi-ISC-1$^{\Delta C}$ were separately fused in-frame to the sequence of yeast invertase without its own SP in the vector pSUC2. The Avr1b SP, which has been reported as a secretory leader in *P. sojae*, was used as a positive control (Gu et al., 2011) and the empty pSUC2 vector was used as a negative control. The fusion constructs were transformed into the invertase secretion-deficient yeast strain YTK12. The results showed that all the transformants grew on CMD−W medium, but only Mi-ISC-1, Mi-ISC-1$^{\Delta C}$, and SP of Avr1b enabled the yeast strain YTK12 to grow on the YPRAA medium. No growth was seen of yeast containing the empty vector pSUC2 or the Mi-ISC-1$^{\Delta N}$ construct. Furthermore, invertase secretion was confirmed with a 2,3,5-triphenyltetrazolium chloride (TTC) assay, which is reduced by monosaccharides to the insoluble red-coloured triphenylformazan. As expected, YTK12 carrying Mi-ISC-1, Mi-ISC-1$^{\Delta C}$, or the Avr1b SP catalysed TTC into the insoluble red compound, and this was not observed in Mi-ISC-1$^{\Delta N}$, empty vector transformants, or untransformed YTK12 (Figure 4). This shows that Mi-ISC-1 is a secretory protein despite lacking a classical N-terminal SP and that the N-terminus of the protein is essential for secretion.

2.5 | The unconventional secretory signal present on Mi-ISC-1 is not recognized by the plant secretory pathway and Mi-ISC-1 is localized within the plant cell

To gain insight into the distribution of Mi-ISC-1 in the plant cell, Mi-ISC-1 fused with GFP was transiently expressed in *N. benthamiana* leaves using *Agrobacterium* infiltration, and the fluorescence signal was observed using confocal microscopy. GFP signals from the fusion protein were visible in both the cytoplasm and the nucleus of plant cells, similar to that from GFP alone. Moreover, no signal from the Mi-ISC-1::GFP fusion was co-localized with the mCherry-tagged pt-rk CD3-999, a marker of the plastids, which is one of the key cellular organelles for SA biosynthesis in plants (Figure 5a).

As the yeast signal sequence trap assay showed that Mi-ISC-1 is a secretory protein despite lacking a classical N-terminal SP, it

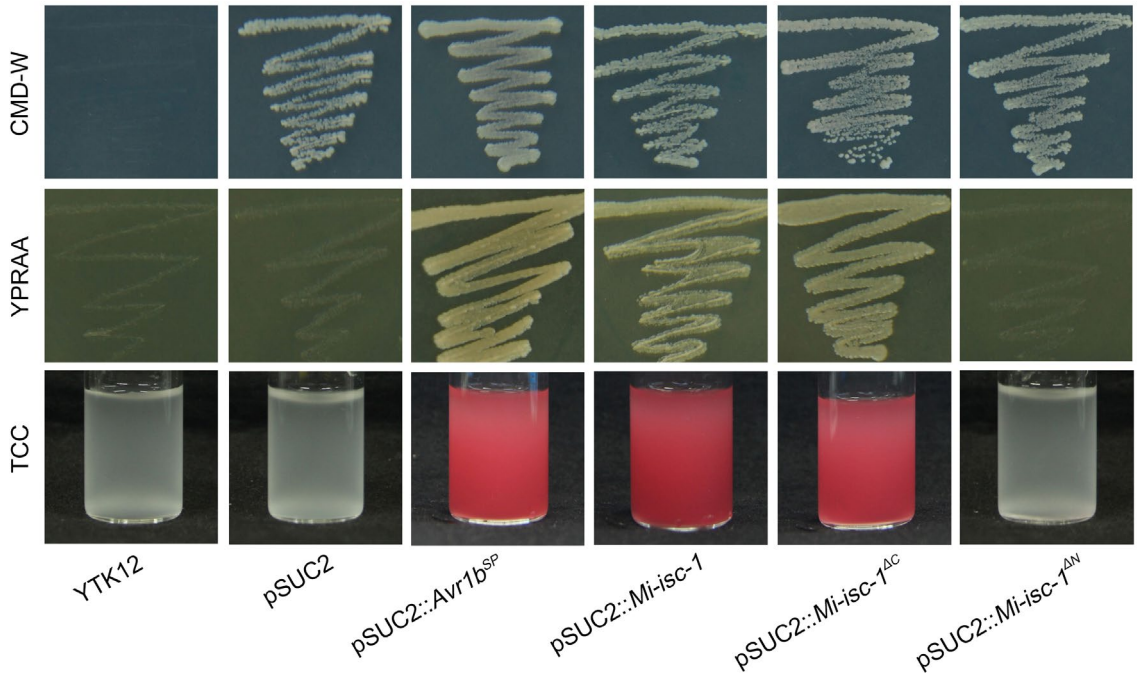

FIGURE 4 Validation of Mi-ISC-1 secretion using the yeast secretion trap assay. The full-length sequence of Mi-ISC-1, and its N- and C-terminal truncated sequences were fused in-frame to the invertase sequence in the pSUC2 vector and transformed into yeast strain YTK12. The untransformed YTK12 strain and empty pSUC2 vector were used as negative controls, and the SP of the effector Avr1b from *Phytophthora sojae* was used as a positive control. Only yeast strains that can secrete invertase can grow on YPRAA medium and change 2,3,5-triphenyltetrazolium chloride (TTC) to red triphenylformazan

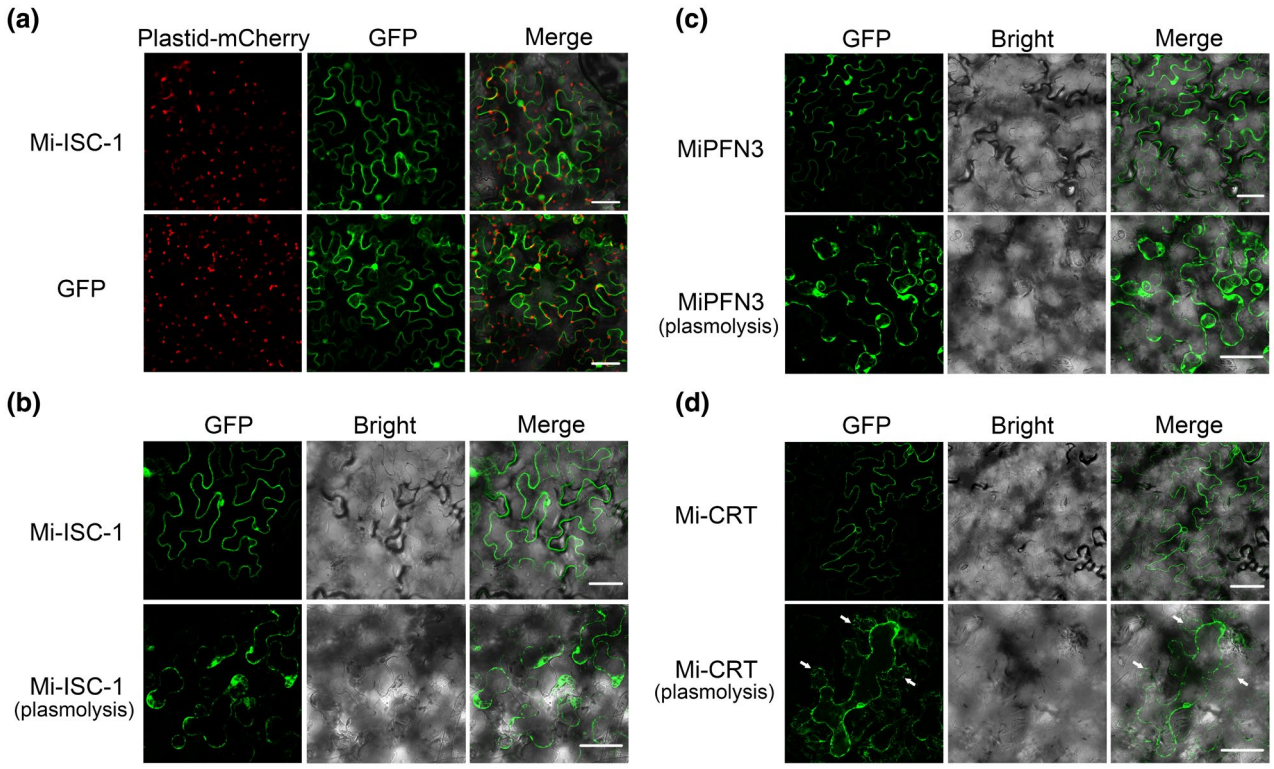

FIGURE 5 Subcellular localization of Mi-ISC-1 in plant cells. (a) The fluorescence signals from Mi-ISC-1 fused to green fluoresecent protein (GFP) was present in both the cytoplasm and the nucleus, which was similar to that of GFP alone, and no co-localization with the mCherry-tagged plastid marker was observed. (b)–(d) The fluorescence signal of transiently expressed proteins in *Nicotiana benthamiana* leaves before and after plasmolysis treatment. Mi-ISC-1 and MiPFN3 were only observed in the cytoplasm and nucleus, but the fluorescence signal of Mi-CRT was also found in the apoplast when the plant leaves were exposed to 1.5 M NaCl for 5 min. The arrows indicate the space after plasmolysis. Photographs were taken 2 days after infiltration and all results shown are representative of three independent experiments. Bar represents 50 μm

was expected that Mi-ISC-1 should be exported to the extracellular space after *Agrobacterium*-mediated expression, rather than localize to the cytoplasm. To confirm the subcellular localization of Mi-ISC-1 in plant cells, a plasmolysis assay was carried out: no signal of Mi-ISC-1::GFP fusion was observed between the cell membrane and cell wall (Figure 5b). It is possible that the sequence allows secretion from the nematode and from yeast cells but does not function within plant cells. To verify this hypothesis, two other full-length coding sequences of *M. incognita* effectors were cloned and analysed. One was Mi-CRT, which contains a predicted N-terminal SP, while the other, MiPFN3, lacks a classical N-terminal SP (Jaouannet et al., 2013; Leelarasamee et al., 2018). Both are secretory proteins that were identified as being present in nematode stylet secretions (Bellafiore et al., 2008; Jaubert et al., 2002). As expected, the yeast invertase secretion assay showed that both Mi-CRT and MiPFN3 can be secreted from yeast cells (Figure S4). However, only Mi-CRT entered the plant secretory pathway where it was co-localized with endoplasmic reticulum (ER) and Golgi markers, and was then secreted to the apoplast in *Agrobacterium*-mediated transient expression assays on *N. benthamiana* leaves, whereas this was not seen for either Mi-ISC-1 or MiPNF3 (Figure S5 and Figure 5b). These results further suggest that the secretory signal present on Mi-ISC-1 and MiPNF3 is different from those present in proteins that contain a classical N-terminal SP and is not recognized by the plant secretory pathway.

2.6 | Mi-ISC-1 suppresses SA-mediated defence in planta and promotes pathogen infection

To further verify the role of Mi-ISC-1 within plant cells, Mi-ISC-1 and the negative control GFP were transiently expressed in *N. benthamiana* leaves via agroinfiltration, and the infiltrated regions were inoculated with the oomycete pathogen *P. capsici* 48 h after infiltration. The *M. incognita* effector Mi-CM-3, which had been demonstrated previously to suppress levels of SA in planta, was used as a positive control (Wang et al., 2018). The expression of all recombinant proteins with expected lengths was confirmed by western blotting using an anti-GFP antibody (Figure 6a). The inoculation assays showed that *N. benthamiana* expressing Mi-ISC-1 or Mi-CM-3 was more susceptible to *P. capsici* infection compared with leaves expressing GFP alone (Figure 6b). The size of the lesions caused by *P. capsici* was found to be significantly increased by 8.7% and 7.0%, respectively (Figure 6c). We further tested whether Mi-ISC-1 directly affects SA accumulation in plant cells during *P. capsici* infection. The results indicated that *N. benthamiana* expressing Mi-ISC-1

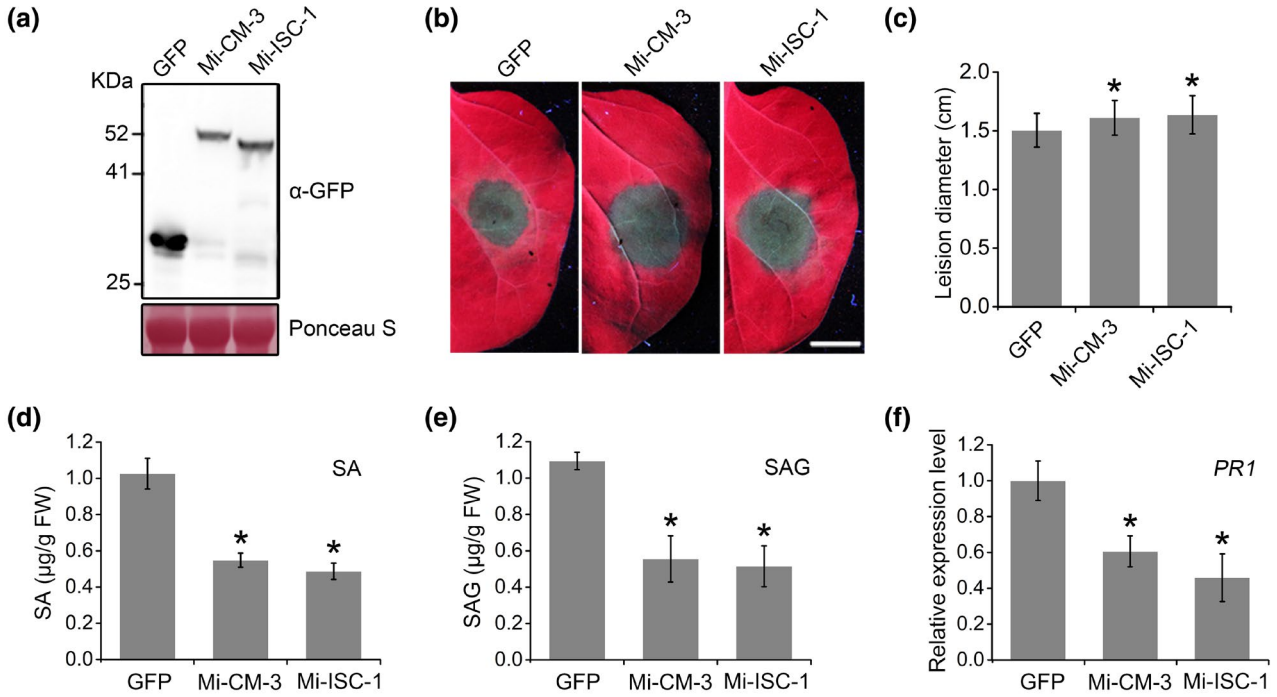

FIGURE 6 Transient expression of Mi-ISC-1 suppresses salicylic acid (SA)-mediated disease resistance. (a) Western blotting of the transiently expressed proteins in *Nicotiana benthamiana* leaves using anti-GFP antibodies. (b) Representative photographs of *N. benthamiana* leaves transiently expressing the indicated genes inoculated with *Phytophthora capsici*. Photographs were taken at 36 h postinoculation (hpi). Bar represents 1 cm. (c) Lesion diameters of inoculated *N. benthamiana* leave at 36 hpi, averaged from three independent biological replicates using at least 18 leaves each. (d) Free salicylic acid (SA) and (e) salicylate glucoside (SAG) levels in *N. benthamiana* leaves at 12 hpi. (f) Relative expression levels of *PR1* gene in *N. benthamiana* leaves at 12 hpi. The data shown were calculated from three independent biological replicates with similar results. Statistically significant differences were determined using a Student's *t* test (*$p <$ 0 .05)

or Mi-CM-3 contained significantly lower levels of SA, resulting in reductions by 52.5% and 46.6% compared with the GFP control, respectively, as well as reductions by 52.9% and 49.2% of salicylate glucoside (SAG) (Figure 6d,e). Furthermore, the expression levels of the SA-associated gene *PR1* were also suppressed following expression of the nematode effectors (Figure 6f). These results provide evidence that Mi-ISC-1 can suppress SA levels and thus mediate plant immunity to promote *P. capsici* infection.

2.7 | The localization of Mi-ISC-1 in the plant cell cytoplasm is required for its virulence

As the results above show that Mi-ISC-1 can suppress SA-mediated plant immunity when it is transiently expressed in plant cells, to determine whether the virulence function of Mi-ISC-1 is associated with its subcellular localization we generated Mi-ISC-1 variants that are fused to a eukaryotic nuclear localization (NLS), a nuclear export (NES), or nonfunctional nls and nes sequences, respectively (Heidrich et al., 2011; Wen et al., 1995). In *Agrobacterium*-mediated transient expression assays of *N. benthamiana* leaves, as expected, the GFP signals from NLS-fused or NES-fused Mi-ISC-1 were detected only in the nucleus or cytoplasm, respectively, whereas those from mutated nls-fused or nes-fused Mi-ISC-1 still displayed a nucleocytoplasmic distribution (Figure 7a). We further inoculated *N. benthamiana* leaves that were agroinfiltrated with these Mi-ISC-1 variants with *P. capsici*. Subsequent analysis showed that the diameters of the lesions caused by *P. capsici* were increased, while the levels of SA, SAG, and *PR1* mRNA were significantly reduced following expression of NES-fused Mi-ISC-1, and mutated nls and nes variants, whereas when Mi-ISC-1 was restricted to the nucleus via fusion to the NLS, the effector no longer suppressed resistance to *P. capsici* or reduced SA, SAG, and *PR1* transcript levels compared with leaves expressing Mi-ISC-1 (Figure 7b). Together, these results indicate that localization of Mi-ISC-1 in the cytoplasm is required for its immune suppression activity.

2.8 | Mi-ISC-1 suppresses the production of SA following de novo reconstruction of the SA biosynthesis pathway in *N. benthamiana*

It has been demonstrated that *PBS3*, *SID1*, and *SID2* of *A. thaliana* is the minimum gene set necessary and sufficient to reconstitute de novo SA biosynthesis via the isochorismate pathway in the cytoplasm of *N. benthamiana* leaves (Torrens-Spence et al., 2019). To determine whether Mi-ISC-1 could affect the production of SA via this reconstituted pathway, these three *A. thaliana* genes were cloned and transiently expressed in *N. benthamiana* leaves using *Agrobacterium* infiltration, and the SA levels were measured using

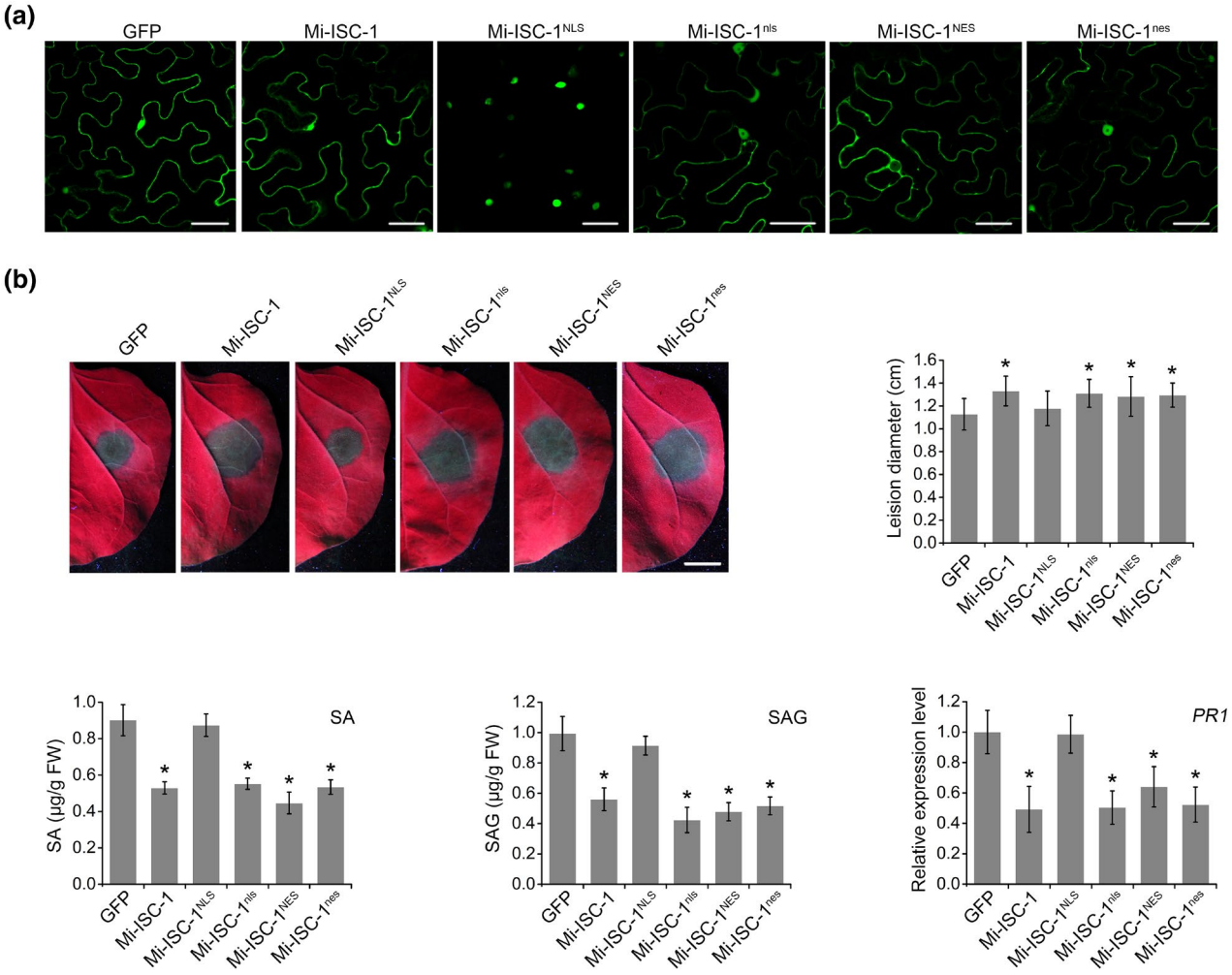

FIGURE 7 Cytoplasmic localization of Mi-ISC-1 is critical for its virulence. (a) Confocal microscopy images showing the subcellular localization of Mi-ISC-1 attached with the nuclear localization signal (NLS) and nuclear export signal (NES), and the mutant forms nls and nes. (b) The effect of subcellular localization of Mi-ISC-1 on plant immunity. Those *Agrobacterium tumefaciens* strains with NES-, nls-, or nes-tagged Mi-ISC-1 can still promote the infection of *Phytophthora capsici* and reduce the salicyclic acid (SA), salicylate glucoside (SAG), and *PR1* transcript levels, but those NLS-tagged Mi-ISC-1 no longer suppress the resistance of *Nicotiana benthamiana* to *P. capsici*. The data shown were calculated from three independent biological replicates with similar results. Statistically significant differences were determined using a Student's *t* test ($p < 0.05$). Bar represents 1 cm

high-performance liquid chromatography (HPLC). As expected, simultaneous co-expression of PBS3, SID1, and SID2 resulted in a significant increase in SA levels compared with expression of PBS3 alone or SID1 and SID2 together in *N. benthamiana* leaves. However, co-expression of Mi-ISC-1 together with PBS3, SID1, and SID2 caused the accumulation of SA to be significantly reduced, while no effect on the de novo SA biosynthesis was detected when GFP was introduced (Figure 8a). These results indicate that Mi-ISC-1 expression in cytoplasm suppresses production of SA following reconstitution of the de novo SA biosynthesis pathway in *N. benthamiana*.

3 | DISCUSSION

Effectors are key pathogen molecules that are secreted into plant cells or the apoplast to manipulate host metabolism. Many effectors suppress immune responses during colonization of a pathogen. Identification and functional characterization of pathogen effectors is important to understand infection mechanisms and the function of the plant immune system, and can also feed into the development of new strategies for plant disease management.

Effectors are typically characterized by the presence of an N-terminal SP for secretion and the lack of an additional transmembrane domain. For plant-parasitic nematodes, they are most often specifically expressed in the oesophageal glands (Mitchum et al., 2013). A variety of effectors have been identified from a range of nematodes that suppress plant immune responses and promote nematode parasitism (e.g., Chen, Lin, et al., 2017; Habash et al., 2017; Naalden et al., 2018; Zhuo et al., 2019). In the current study, we demonstrated that a sedentary endoparasite *M. incognita* deploys a functional ISC effector to disrupt the SA metabolism pathway. Bioinformatic analysis indicated that a canonical SP is absent from

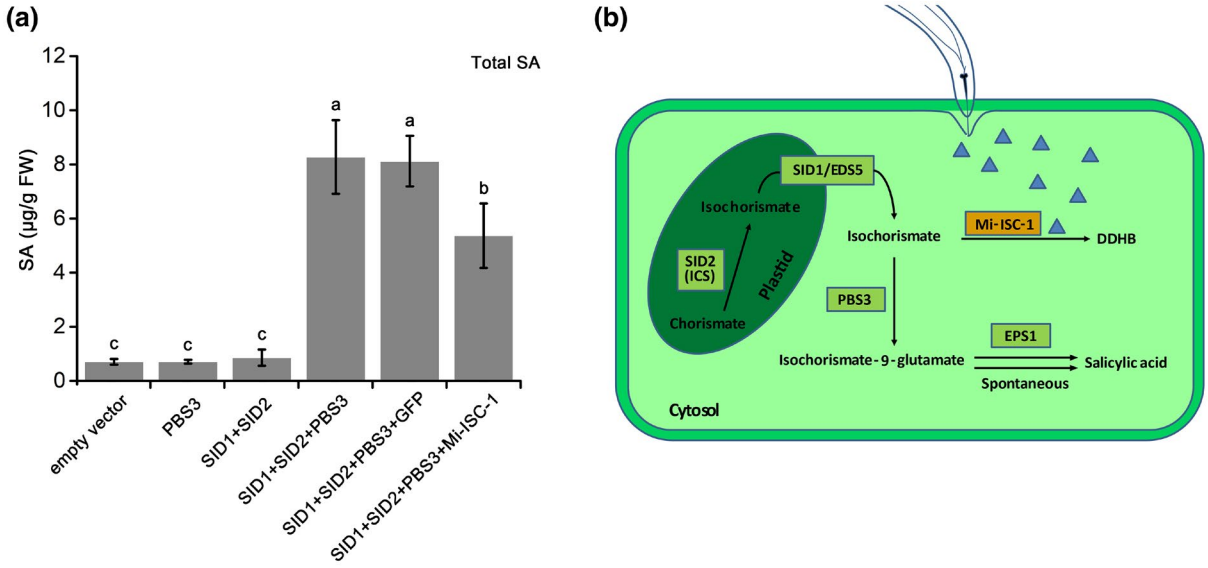

FIGURE 8 Mi-ISC-1 disrupts salicylic acid (SA) synthesis in host plants. (a) Mi-ISC-1 affects the production of SA via the reconstitution of de novo SA biosynthesis in *Nicotiana benthamiana*. Quantification of SA in various co-infiltrated *N. benthamiana* leaves at 4 days postinfiltration (dpi). The data shown were calculated from three independent biological replicates with similar results. Statistically significant differences using one-way analysis of variance followed by Tukey's tests ($p < 0.05$) are indicated with different letters. (b) Proposed model of Mi-ISC-1 subverting plant SA biosynthesis to suppress plant immunity. Chorismate is converted to isochorismate in the plastid by isochorismate synthase (ICS) SID2, then the isochorismate is transported by EDS5 (earlier named SID1) to the cytosol, where the isochorismoyl-glutamate synthase PBS3 catalyses the conjugation of L-glutamate to isochorismate to produce isochorismate-9-glutamate, which is then converted to SA by EPS1 or spontaneous decay. *Meloidogyne incognita* secretes Mi-ISC-1 to compete with PBS3 to deplete the cytoplasmic isochorismate, thus disrupting SA biosynthesis via the ICS pathway

the amino acid sequence of Mi-ISC-1. However, the expression of the gene encoding this protein in the subventral gland cells, coupled to the fact that the substrates for the activity of this protein are absent in nematodes, suggested a role in the plant–nematode interaction. Enzyme activity assays further confirmed that Mi-ISC-1 can metabolize isochorismate into DDHB and pyruvate, and thus may deplete the central precursor for SA biosynthesis in host plants.

Generally, secretory proteins in eukaryotic cells are transported through the conventional ER-to-Golgi membrane pathway. In brief, SP-bearing proteins are translocated into the lumen of the ER for processing and modification, then delivery to the Golgi apparatus. Eventually, the secretory cargos are released into the extracellular matrix across the plasma membrane (Lee et al., 2004). The majority of nematode effectors identified previously are secreted from the nematode following this paradigm (Siddique & Grundler, 2018). However, four exceptions have been described, including direct translocation through lipidic pores in the plasma membrane, secretion via ATP-binding-cassette (ABC) transporter proteins, and uptake into endocytic compartments followed by fusion with the plasma membrane and inserting in the ER membrane but bypassing the Golgi (Dimou & Nickel, 2018). In the present study, we demonstrated that Mi-ISC-1, which lacks a canonical SP, guides invertases for secretion from yeast cells. Therefore, Mi-ISC-1 may be an unconventionally secreted protein, although the exact translocation mechanism underlying its secretion is yet to be determined. Analysis of deduced amino acid sequences that include an isochorismatase domain from genome data of root-knot nematodes and cyst nematodes showed that these ISC-like proteins can be divided into two groups based on amino acid sequence similarity (Figure S6). In addition, all lack a classical N-terminal SP (Table S2). It is not clear whether these proteins evolved from a common ancestor that is an unconventionally secreted protein or whether all SPs were lost under similar selective pressure.

Further subcellular localization observations and plasmolysis assays showed that Mi-ISC-1 was localized within the cytoplasm when it was transiently expressed in *N. benthamiana* leaves by agroinfiltration. The localization of Mi-ISC-1 was similar to that of another nematode secretory protein, MiPFN3, that also lacks a classical N-terminal SP. By contrast, the nematode effector Mi-CRT, with an SP, was secreted to the apoplast following *Agrobacterium*-mediated transient expression assays on *N. benthamiana* leaves. These results revealed that the unconventional secretory signal sequence present on Mi-ISC-1 is not recognized by the plant secretory pathway, thus allowing the effector to be retained in the cytoplasm. Ectopic expression and *P. capsici* infection assays further confirmed that Mi-ISC-1 suppresses SA-mediated plant immunity and the cytoplasmic localization is required for its virulence.

Mi-ISC-1 was localized within the cytoplasm but not in the plastid of *N. benthamiana* cells. SA was previously thought to be synthesized mainly in the plastids of the plant cell, including through the PAL pathway that converts phenylalanine to *trans*-cinnamic acid as an alternative precursor of SA, and the ICS pathway that produces SA from chorismate through two reactions catalysed by ICS and IPL, although a plant IPL has not yet been identified (Dempsey et al., 2011;

Mustafa et al., 2009; Strawn et al., 2007; Wildermuth et al., 2001). Therefore, when the cytoplasmic CM secreted by *U. maydis* was identified, it was proposed that the fungal enzyme increases the flow of chorismate from the plastid to the cytosol by depletion of the cytoplasmic pool and thus reduces the available substrate for SA biosynthesis in plastids (Djamei et al., 2011). A similar mechanism was used to explain how pathogen-derived ISC effectors act on the ICS pathway of SA biosynthesis in the plant. *P. sojae* and *V. dahliae* secrete isochorismatases (PsIsc1 and VdIsc1, respectively) into the cytosol where they deplete the isochorismate, thus enhancing its export from the plastid, resulting in the reduction of SA biosynthesis in plastids (Liu et al., 2014).

However, an important milestone in SA biosynthesis of the plant recently revealed that the cytosol itself is a key compartment for the pathogen-induced SA biosynthesis pathway in plants. First, chorismate is converted to isochorismate in the chloroplast by ICS and subsequently exported to the cytoplasm via the chloroplast membrane proteins EDS5 or SID1. PBS3 (avrPphB Susceptible 3) subsequently catalyses the conjugation of L-glutamate to isochorismate to produce isochorismate-9-glutamate and, finally, SA is produced by EPS1 or spontaneous decay. Thus, co-expression of the three proteins PBS3, SID1, and SID2 of *A. thaliana* is sufficient to reconstitute de novo SA biosynthesis in *N. benthamiana* (Rekhter et al., 2019; Torrens-Spence et al., 2019). In the present study, we demonstrated that the cytoplasmic effector Mi-ISC-1 was able to suppress the production of SA when it was co-expressed with these three *A. thaliana* proteins. In consideration of the ISC activity that catalyses the hydrolysis of isochorismate into DDHB, and the virulence function of Mi-ISC-1 in plant cytoplasm, we propose that the nematode effector may divert the cytoplasmic isochorismate away from conjugation to L-glutamate, thus directly interrupting SA biosynthesis in the cytosol, rather than depleting isochorismate in the plastid (Figure 8b).

Combined with our previous report (Wang et al., 2018), we conclude that *M. incognita* may use CM and ISC effectors targeting chorismate and isochorismate, respectively, to disrupt SA biosynthesis and thus plant defence responses. CM effectors may not only affect the synthesis of SA, but also the auxin indole-3-acetic acid (IAA), which is derived from chorismate via the amino acid tryptophan (Doyle & Lambert, 2003; Wang et al., 2018), However, the substrate of isochorismatase is isochorismate, which is a downstream product of chorismate, suggesting that the nematode ISC effector may exclusively impair SA biosynthesis in the plant. In summary, the results suggest that Mi-ISC-1 may play an important role in manipulating plant immunity to promote nematode parasitism.

4 | EXPERIMENTAL PROCEDURES

4.1 | Nematodes and plants

M. incognita nematodes isolated from Jiangsu, China, were routinely maintained on tomato plants (cv. Sufen No. 8) in a greenhouse at 25°C. Egg masses were handpicked from the galled roots and hatched to preparasitic second-stage juveniles (pre-J2s) after incubating in water at 25°C in modified Baermann pans for 2–3 days. Different parasitic stages of juveniles and females were collected as previously described (Huang et al., 2005). *P. capcisi* strains were cultured on 10% vegetable (V8) juice medium at 25°C in the dark. Seedlings of *N. benthamiana* were grown in a greenhouse at 23°C under a 16-h light/8-h dark cycle.

4.2 | Nucleic acid extraction and gene cloning

M. incognita genomic DNA and total RNA were extracted from freshly hatched pre-J2s using the E.Z.N.A. Mollusc DNA Kit (Omega) and RNAgents Total RNA Isolation System Kit (Promega), respectively. Complementary DNA (cDNA) was synthesized from total RNA using PowerScript reverse transcriptase (Clontech) according to the manufacturer's instructions. The coding sequence of *Mi-isc-1* and its genomic clone was obtained by PCR amplification using primer set IscLg-F/IscLg-R, which was designed from a coding sequence (Minc12702) deposited in the WormBase database. PCR products were purified using a Cycle-Pure Kit (Omega) and the fragments were ligated with the pMD19-T vector (Takara) and then transformed into *E. coli* DH5α competent cells for sequencing. All primers used in this study are listed in Table S1 and were synthesized by TsingKe Biotechnology Co. Ltd.

4.3 | Bioinformatic analysis

The whole-genome and protein sequences of *M. incognita* were downloaded from the WormBase database (http://www.wormbase.org/). Prediction of the SP for secretion was performed using SignalP v. 5.0 (http://www.cbs.dtu.dk/services/SignalP/). Conserved domains were predicted using the Pfam 33.1 database (Mistry et al., 2021). The sequence similarity of the predicted proteins was analysed using BLASTP and BLASTX searches (Altschul et al., 1997). Multiple amino acid sequences were aligned with ClustalW v. 1.82 (Thompson et al., 1994). The secondary structures were predicted using the MPI Bioinformatics Toolkit (Zimmermann et al., 2018).

4.4 | mRNA in situ hybridization and developmental expression analysis

A 465 bp fragment of *Mi-isc-1* was amplified from *M. incognita* pre-J2 cDNA using the primer pair IscIH-F and IscIH-R. The PCR product was used to synthesize DIG-labelled sense and antisense single-stranded cDNA probes using the PCR DIG Probe Synthesis kit (Roche) by asymmetric PCR (Gyllensten & Erlich, 1988). In situ hybridization was performed with pre-J2 and mixed parasitic stages of *M. incognita* as described previously (De Boer et al., 1998). Hybridization signals within the nematodes were detected using an alkaline phosphatase-conjugated anti-DIG antibody and visualized

with the colourimetric substrates NBT/BCIP. The specimens were observed under a BX51 microscope (Olympus).

Total RNA of eggs and nematodes at different life stages were extracted separately as described above. Transcripts of *Mi-isc-1* from different developmental stages of *M. incognita* were detected by RT-qPCR with primer pair IscRT-F/IscRT-R. The *actin* gene (Minc06769) used as a control was amplified synchronously from each sample with primers MiactF/MiactR. RT-qPCR was performed using SYBR premix ExTaq (Abm) on an Applied Biosystems QS6 system (Applied Biosystems). The relative transcript levels of *Mi-isc-1* in each sample were normalized using the *actin* gene and calculated using the $2^{-\Delta\Delta Ct}$ method (Pfaffl, 2001). Three independent biological replicates were performed and each reaction was run in triplicate.

4.5 | In planta RNAi

TRV-mediated gene silencing was conducted as previously described (Liu et al., 2002). A 520 bp fragment of the *Mi-isc-1* gene was amplified with the primer pairs IscTRV-F/IscTRV-R and then cloned into *Bam*HI and *Xho*I sites of pTRV2 to generate vector pTRV2::*Mi-isc-1*. The vectors pTRV1 and pTRV2::*Mi-isc-1*, as well as negative control pTRV2::*gfp* were transferred into *Agrobacterium tumefaciens* GV3101 by electroporation. Tomato plants were infiltrated with *A. tumefaciens* carrying the relevant constructs as previously described (Dubreuil et al., 2009). The TRV coat protein gene in tomato roots was detected at 3, 7, 14, and 21 days postinfiltration by RT-PCR using primers TRV-cp-F/TRV-cp-R, using *GAPDH* as an RNA reference gene. To assess the effect of *Mi-isc-1* silencing on nematode parasitism, 10 TRV tomato lines at 21 dpi and/or noninfiltrated tomato plants were inoculated with 250 pre-J2 nematodes. The roots were harvested at 45 dpi, washed, and stained with trypan blue. The numbers of galls and egg masses were counted in each plant. Three independent experiments were performed.

To test the silencing efficiency, 200 parasitic stage nematodes were collected from each tomato line at 14 days postinoculation (dpi) for RNA extraction. Each treatment was sampled three times and the expression level changes of *Mi-isc-1* were analysed by RT-qPCR as described above. Data were analysed by SPSS v. 19.0 and statistically significant differences between each treatment were determined by Duncan's multiple range test.

4.6 | Yeast secretion trap assay

The vector pSUC2T7M13ORI (pSUC2), which carries a truncated invertase gene (*SUC2*) lacking the SP coding sequence, was used in this assay (Jacobs et al., 1997). The coding sequences of *Mi-CRT* (AF402771), *MiPFN3* (MW345915), *Mi-isc-1*, and the truncated mutants lacking the N or C terminus were amplified and ligated into pSUC2 vector using *Eco*RI and *Xho*I enzyme sites. The pSUC2-derived plasmids were transformed into the invertase-deficient yeast strain YTK12 by the lithium acetate method (Gietz et al., 1995). The untransformed YTK12 strain and YTK12 strains transformed with pSUC2 empty vector were used as negative controls, and the strain transformed with pSUC2 vector fused with the predicted SP of the oomycete effector Avr1b was used as a positive control (Shan et al., 2004). A tryptophan-deficient medium CMD−W (0.67% yeast N base without amino acids, 0.075% W dropout supplement, 2% sucrose, 0.1% glucose, and 2% agar) was used to select YTK12 strains containing the empty pSUC2 vector or pSUC2-derived constructs. Then the transformants were plated on the YPRAA plates (1% yeast extract, 2% raffinose, 2% peptone, and 2 mg/ml antimycin A) to detect invertase secretion. Invertase enzymatic activity was also confirmed by an increase in insoluble red-coloured triphenylformazan due to the reduction of TTC (Oh et al., 2009).

4.7 | Enzyme activity assays and measurement of DDHB content

The coding sequence of three enzymes (EntA, EntB, EntC) that are necessary for the conversion of chorismate to 2,3-dihydroxybenzoate via isochorismate in bacteria were amplified from *E. coli* JM109 (Liu et al., 1989, 1990; Rusnak et al., 1989). The amplified genes were separately cloned into pET28a (Novagen) and the plasmids were transformed into *E. coli* BL21 (DE3). Protein expression in BL21 (DE3) cells was induced by adding 1 mM isopropyl-β-D-1-thiogalactopyranoside (IPTG) at 18°C for 10 h and purified using HisTrap HP according to the manufacturer's instructions (GE Healthcare). The purified proteins were detected by SDS-PAGE followed by Coomassie Brilliant blue staining. Mi-ISC-1, as well as negative control GFP proteins, was transiently expressed in *N. benthamiana* and purified as described above.

Measurement of the isochorismatase activity of Mi-ISC-1 was performed in two steps as described previously (Liu et al., 2012). First, the conversion of chorismate to isochorismate was performed in a total volume of 100 μl containing 20 mM chorismate, 100 mM phosphate-buffered saline (PBS) pH 7.0, 10 mM $MgCl_2$, and 0.85 μg of *E. coli* EntC at room temperature for 2 h. Second, 5 μl of reaction solution from the first step, 0.06 μg of Mi-ISC-1, and 3.8 μg of purified EntA was mixed in a total volume of 50 μl containing 100 mM PBS pH 7.0, 0.8 mM NAD^+. The purified *E. coli* isochorismatase, EntB, was used as a positive control and GFP as a negative control. The enzyme activity was then determined by measuring the increase in absorbance at 340 nm owing to NAD^+ reduction using an Uvikon spectrophotometer.

4.8 | Measurement of SA/SAG concentrations and *PR1* gene expression

The coding sequence of *Mi-isc-1*, and variants fused with a nuclear localization signal (NLS), nuclear export signal (NES), and corresponding mutants nls and nes at the N terminus of *Mi-isc-1* were ligated into the pCAMBIA1300-eGFP vector to express the relevant

eGFP fusion proteins. The recombinant vectors were introduced into *A. tumefaciens* GV3101 and transiently expressed in *N. benthamiana* by agroinfiltration for virulence analysis. The *M. incognita* effector Mi-CM-3, which has been demonstrated to suppress SA-mediated immunity, was used as a positive control (Wang et al., 2018) and GFP as a negative control. Leaves of *N. benthamiana* were inoculated with *P. capsici* 48 h after *Agrobacterium* infiltration as described previously (Yu et al., 2012), the concentrations of free SA and conjugated SAG were detected at 12 hpi in infected leaves using HPLC as described by Lee et al. (2011), and the relative levels of *PR1* gene were also measured as described by Rajput et al. (2014). Lesion diameters caused by *P. capsici* infection were photographed and measured at 36 hpi.

4.9 | Confocal microscopy

The coding sequences of *Mi-CRT* and *Mi-PFN3* were ligated into pCAMBIA1300-eGFP vector and then introduced into *A. tumefaciens* GV3101. All the GFP-tagged proteins, including those Mi-ISC-1 fused with NES, nes, NLS, or nls peptides, were transiently expressed in *N. benthamiana* leaves by agroinfiltration. The plasmid pt-rk CD3-999 with mCherry was used as a plastid localization marker for subcellular localization (Nelson et al., 2007). Leaf discs were taken at 2 dpi from the infiltrated area of *N. benthamiana* leaves and observed using an LSM 710 confocal microscope (Zeiss Microsystems). RFP or GFP fluorescence was detected at an excitation wavelength of 488 or 561 nm, respectively. A plasmolysis assay was performed as described previously (Nie et al., 2018). Plant leaves were exposed to 1.5 M NaCl for 5 min before observation.

4.10 | Protein extraction and western blot analysis

Leaves of *N. benthamiana* infiltrated with *A. tumefaciens* were collected at 2 dpi and the total protein was extracted using extraction buffer (100 mM Tris-HCl, pH 7.5, 5 mM EDTA, 150 mM NaCl, 1 mM phenylmethylsulfonyl fluoride, 10 mM dithiothreitol, 0.5% Triton X-100, 2% polyvinylpolypyrrolidone, and 1× Roche Complete protein inhibitor tablets). A western blot assay was performed with the samples as described previously (Wang et al., 2018). Membranes were probed with primary mouse anti-His or anti-GFP tag monoclonal antibody (1:3000) (Sigma-Aldrich), followed by goat anti-mouse horseradish peroxidase-conjugated secondary antibody (1:10,000). The protein bands were detected using a BeyoECL STAR Western kit (Beyotime) following the manufacturer's instructions.

4.11 | Reconstitution of de novo SA biosynthesis in *N. benthamiana*

The de novo SA biosynthesis in *N. benthamiana* using *PBS3*, *SID1*, and *SID2* of *A. thaliana* was performed as described by Torrens-Spence et al. (2019). Briefly, the coding sequences of *PBS3*, *SID1*, and *SID2* were amplified using the primers shown in Table S1. The amplified fragments were sequenced and subcloned into the corresponding sites of pCAMBIA1300-His vector and introduced into *A. tumefaciens* GV3101. *A. tumefaciens* carrying the relevant constructs including Mi-ISC-1 and negative GFP, alone or mixed in equal concentrations to a final OD_{600} of 0.3, were then infiltrated into leaves of *N. benthamiana* plants, and the concentrations of total SA were detected as described above.

ACKNOWLEDGEMENTS

We thank Kewei Zhang (Zhejiang Normal University) and Pei Wang (Nanjing Agricultural University) for providing critical reagents. This work was supported by the National Natural Science Foundation of China (31872923 and 31371922). J.J. receives funding from the Scottish Government Rural and Environmental Science and Analytical Services Division.

CONFLICT OF INTEREST

The authors declare no competing interests.

DATA AVAILABILITY STATEMENT

The data that support the findings of this study are available from the corresponding author upon reasonable request.

ORCID

John Jones https://orcid.org/0000-0003-2074-0551
Xuan Wang https://orcid.org/0000-0001-7405-8377

REFERENCES

Altschul, S.F., Madden, T.L., Schäffer, A.A., Zhang, J., Zhang, Z., Miller, W. et al. (1997) Gapped BLAST and PSIBLAST: a new generation of protein database search programs. *Nucleic Acids Research*, 25, 3389–3402.

Bauters, L., Kyndt, T., De Meyer, T., Morreel, K., Boerjan, W. & Lefevere, H. (2020) Chorismate mutase and isochorismatase, two potential effectors of the migratory nematode *Hirschmanniella oryzae*, increase host susceptibility by manipulating secondary metabolite content of rice. *Molecular Plant Pathology*, 21, 1634–1646.

Bellafiore, S., Shen, Z., Rosso, M.N., Abad, P., Shih, P. & Briggs, S.P. (2008) Direct identification of the *Meloidogyne incognita* secretome reveals proteins with host cell reprogramming potential. *PLoS Pathogens*, 4, e1000192.

de Boer, J.M., Yan, Y., Smant, G., Davis, E.L. & Baum, T.J. (1998) In-situ hybridization to messenger RNA in *Heterodera glycines*. *Journal of Nematology*, 30, 309–312.

Caillaud, M.C., Asai, S., Rallapalli, G., Piquerez, S., Fabro, G. & Jones, J.D.G. (2013) A downy mildew effector attenuates salicylic acid-triggered immunity in Arabidopsis by interacting with the host mediator complex. *PLoS Biology*, 11, e1001732.

Caruthers, J., Zucker, F., Worthey, E., Myler, P.J., Buckner, F., Van Voorhuis, W. et al. (2005) Crystal structures and proposed structural/functional classification of three protozoan proteins from the isochorismatase superfamily. *Protein Science*, 14, 288–2894.

Chen, H., Chen, J., Li, M., Chang, M., Xu, K., Shang, Z. et al. (2017) A bacterial type III effector targets the master regulator of salicylic acid signaling, NPR1, to subvert plant immunity. *Cell, Host and Microbe*, 22, 777–788.e7.

Chen, J., Lin, B., Huang, Q., Hu, L., Zhuo, K. & Liao, J. (2017) A novel *Meloidogyne graminicola* effector, MgGPP, is secreted into host cells and undergoes glycosylation in concert with proteolysis to suppress plant defenses and promote parasitism. *PLoS Pathogens*, 13, e1006301.

Dempsey, D.A., Vlot, A.C., Wildermuth, M.C. & Klessig, D.F. (2011) Salicylic acid biosynthesis and metabolism. *The Arabidopsis Book*, 9, e0156.

Dimou, E. & Nickel, W. (2018) Unconventional mechanisms of eukaryotic protein secretion. *Current Biology*, 28, R406–R410.

Djamei, A., Schipper, K., Rabe, F., Ghosh, A., Vincon, V., Kahnt, J. et al. (2011) Metabolic priming by a secreted fungal effector. *Nature*, 478, 395–398.

Doyle, E.A. & Lambert, K.N. (2003) *Meloidogyne javanica* chorismate mutase 1 alters plant cell development. *Molecular Plant-Microbe Interactions*, 16, 123–131.

Drake, E.J., Nicolai, D.A. & Gulick, A.M. (2006) Structure of the EntB multidomain nonribosomal peptide synthetase and functional analysis of its interaction with the EntE adenylation domain. *Chemistry and Biology*, 13, 409–419.

Dubreuil, G., Magliano, M., Dubrana, M.P., Lozano, J., Lecomte, P., Favery, B. et al. (2009) Tobacco rattle virus mediates gene silencing in a plant parasitic root-knot nematode. *Journal of Experimental Botany*, 60, 4041–4050.

Elling, A.A. (2013) Major emerging problems with minor *Meloidogyne* species. *Phytopathology*, 103, 1092–1102.

Fu, Z.Q. & Dong, X. (2013) Systemic acquired resistance: turning local infection into global defense. *Annual Review of Plant Biology*, 64, 839–863.

Gietz, R.D., Graham, K.C. & Litchfield, D.W. (1995) Interactions between the subunits of casein kinase II. *Journal of Biological Chemistry*, 270, 13017–13021.

Gleason, C., Polzin, F., Habash, S.S., Zhang, L., Utermark, J., Grundler, F.M.W. et al. (2017) Identification of two *Meloidogyne hapla* genes and an investigation of their roles in the plant–nematode interaction. *Molecular Plant-Microbe Interactions*, 30, 101–112.

Goral, A.M., Tkaczuk, K.L., Chruszcz, M., Kagan, O., Savchenko, A. & Minor, W. (2012) Crystal structure of a putative isochorismatase hydrolase from *Oleispira antarctica*. *Journal of Structural and Functional Genomics*, 13, 27–36.

Gu, B., Kale, S.D., Wang, Q., Wang, D., Pan, Q., Cao, H. et al. (2011) Rust secreted protein Ps87 is conserved in diverse fungal pathogens and contains a RXLR-like motif sufficient for translocation into plant cells. *PLoS One*, 6, e27217.

Gyllensten, U.B. & Erlich, H.A. (1988) Generation of single-stranded DNA by the polymerase chain reaction and its application to direct sequencing of the HLA-DQA locus. *Proceedings of the National Academy of Sciences of the United States of America*, 85, 7652–7656.

Habash, S.S., Radakovic, Z.S., Vankova, R., Siddique, S., Dobrev, P., Gleason, C. et al. (2017) *Heterodera schachtii* tyrosinase-like protein-a novel nematode effector modulating plant hormone homeostasis. *Scientific Reports*, 7, 6874.

Heidrich, K., Wirthmueller, L., Tasset, C., Pouzet, C., Deslandes, L. & Parker, J.E. (2011) *Arabidopsis* EDS1 connects pathogen effector recognition to cell compartment-specific immune responses. *Science*, 334, 1401–1404.

Huang, G., Dong, R., Allen, R., Davis, E.L., Baum, T.J. & Hussey, R.S. (2005) Two chorismate mutase genes from the root-knot nematode *Meloidogyne incognita*. *Molecular Plant Pathology*, 6, 23–30.

Jacobs, K.A., Collins-Racie, L.A., Colbert, M., Duckett, M., Golden-Fleet, M., Kelleher, K. et al. (1997) A genetic selection for isolating cDNAs encoding secreted proteins. *Gene*, 198, 289–296.

Jaouannet, M., Magliano, M., Arguel, M.J., Gourgues, M., Evangelisti, E., Abad, P. et al. (2013) The root-knot nematode calreticulin Mi-CRT is a key effector in plant defense suppression. *Molecular Plant-Microbe Interactions*, 26, 97–105.

Jaubert, S., Ledger, T.N., Laffaire, J.B., Piotte, C., Abad, P. & Rosso, M.N. (2002) Direct identification of stylet secreted proteins from root-knot nematodes by a proteomic approach. *Molecular and Biochemical Parasitology*, 121, 205–211.

Jones, J.D.G. & Dangl, J.L. (2006) The plant immune system. *Nature*, 444, 323–329.

Kud, J., Wang, W., Gross, R., Fan, Y., Huang, L.I., Yuan, Y. et al. (2019) The potato cyst nematode effector RHA1B is a ubiquitin ligase and uses two distinct mechanisms to suppress plant immune signaling. *PLoS Pathogens*, 15, e1007720.

Lambert, K.N., Allen, K.D. & Sussex, I.M. (1999) Cloning and characterization of an esophageal-gland-specific chorismate mutase from the phytoparasitic nematode *Meloidogyne javanica*. *Molecular Plant-Microbe Interactions*, 12, 328–336.

Lee, D.H., Choi, H.W. & Hwang, B.K. (2011) The pepper E3 ubiquitin ligase RING1 gene, CaRING1, is required for cell death and the salicylic acid-dependent defense response. *Plant Physiology*, 156, 2011–2025.

Lee, M.C., Miller, E.A., Goldberg, J., Orci, L. & Schekman, R. (2004) Bi-directional protein transport between the ER and Golgi. *Annual Review of Cell and Developmental Biology*, 20, 87–123.

Leelarasamee, N., Zhang, L. & Gleason, C. (2018) The root-knot nematode effector MiPFN3 disrupts plant actin filaments and promotes parasitism. *PLoS Pathogens*, 14, e1006947.

Liu, J., Duncan, K. & Walsh, C.T. (1989) Nucleotide sequence of a cluster of *Escherichia coli* enterobactin biosynthesis genes: identification of *entA* and purification of its product 2,3-dihydro-2,3-dihydroxybenzoate dehydrogenase. *Journal of Bacteriology*, 171, 791–798.

Liu, J., Quinn, N., Berchtold, G.A. & Walsh, C.T. (1990) Overexpression, purification, and characterization of isochorismate synthase (EntC), the first enzyme involved in the biosynthesis of enterobactin from chorismate. *Biochemistry*, 29, 1417–1425.

Liu, S., Zhang, C., Li, N., Niu, B., Liu, M., Liu, X. et al. (2012) Structural insight into the ISC domain of VibB from *Vibrio cholerae* at atomic resolution: a snapshot just before the enzymatic reaction. *Acta Crystallographica, Section D, Biological Crystallography*, 68, 1329–1338.

Liu, T., Song, T., Zhang, X., Yuan, H., Su, L., Li, W. et al. (2014) Unconventionally secreted effectors of two filamentous pathogens target plant salicylate biosynthesis. *Nature Communications*, 5, 4686.

Liu, Y., Schiff, M. & Dinesh-Kumar, S.P. (2002) Virus-induced gene silencing in tomato. *The Plant Journal*, 31, 777–786.

Long, H., Wang, X. & Xu, J. (2006) Molecular cloning and life-stage expression pattern of a new chorismate mutase gene from the root-knot nematode *Meloidogyne arenaria*. *Plant Pathology*, 55, 559–563.

Mei, Y., Thorpe, P., Guzha, A., Haegeman, A., Blok, V.C., MacKenzie, K. et al. (2015) Only a small subset of the SPRY domain gene family in *Globodera pallida* is likely to encode effectors, two of which suppress host defences induced by the potato resistance gene *Gpa2*. *Nematology*, 17, 409–424.

Mistry, J., Chuguransky, S., Williams, L., Qureshi, M., Salazar, G., Sonnhammer, E.L.L. et al. (2021) Pfam: the protein families database in 2021. *Nucleic Acids Research*, 49, D412–D419.

Mitchum, M.G., Hussey, R.S., Baum, T.J., Wang, X., Elling, A.A., Wubben, M. et al. (2013) Nematode effector proteins: an emerging paradigm of parasitism. *New Phytologist*, 199, 879–894.

Mustafa, N.R., Kim, H.K., Choi, Y.H., Erkelens, C., Lefeber, A.W.M., Spijksma, G. et al. (2009) Biosynthesis of salicylic acid in fungus elicited *Catharanthus roseus* cells. *Phytochemistry*, 70, 532–539.

Naalden, D., Haegeman, A., de Almeida-Engler, J., Birhane Eshetu, F., Bauters, L. & Gheysen, G. (2018) The *Meloidogyne graminicola* effector Mg16820 is secreted in the apoplast and cytoplasm to

suppress plant host defense responses. *Molecular Plant Pathology*, 19, 2416–2430.

Nelson, B.K., Cai, X. & Nebenführ, A. (2007) A multicolored set of in vivo organelle markers for co-localization studies in Arabidopsis and other plants. *The Plant Journal*, 51, 1126–1136.

Nie, J., Yin, Z., Li, Z., Wu, Y. & Huang, L. (2018) A small cysteine-rich protein from two kingdoms of microbes is recognized as a novel pathogen-associated molecular pattern. *New Phytologist*, 222, 995–1011.

Oh, S.K., Young, C., Lee, M., Oliva, R., Bozkurt, T.O., Cano, L.M. et al. (2009) In planta expression screens of *Phytophthora infestans* RXLR effectors reveal diverse phenotypes, including activation of the *Solanum bulbocastanum* disease resistance protein Rpi-blb2. *The Plant Cell*, 21, 2928–2947.

Pfaffl, M.W. (2001) A new mathematical model for relative quantification in real-time RT-PCR. *Nucleic Acids Research*, 29, e45.

Rajput, N.A., Zhang, M., Ru, Y., Liu, T., Xu, J., Liu, L.I. et al. (2014) *Phytophthora sojae* effector PsCRN70 suppresses plant defenses in *Nicotiana benthamiana*. *PLoS One*, 9, e98114.

Reddy, P.P. (2021) Nematode diseases of crop plants: an overview. In: Reddy, P.P. (Ed.) *Nematode diseases of crops and their management*. Singapore: Springer, pp. 3–32.

Rekhter, D., Lüdke, D., Ding, Y., Feussner, K., Zienkiewicz, K., Lipka, V. et al. (2019) Isochorismate-derived biosynthesis of the plant stress hormone salicylic acid. *Science*, 365, 498–502.

Rusnak, F., Faraci, W.S. & Walsh, C.T. (1989) Subcloning, expression, and purification of the enterobactin biosynthetic enzyme, 3-dihydroxybenzoate-AMP ligase: demonstration of enzyme-bound (2,3-dihydroxybenzoyl) adenylate product. *Biochemistry*, 28, 6827–6835.

Shan, W.X., Cao, M., Dan, L.U. & Tyler, B.M. (2004) The *Avr1b* locus of *Phytophthora sojae* encodes an elicitor and a regulator required for avirulence on soybean plants carrying resistance gene *Rps1b*. *Molecular Plant-Microbe Interactions*, 17, 394–403.

Siddique, S. & Grundler, F.M.W. (2018) Parasitic nematodes manipulate plant development to establish feeding sites. *Current Opinion in Microbiology*, 46, 102–108.

Strawn, M.A., Marr, S.K., Inoue, K., Inada, N., Zubieta, C. & Wildermuth, M.C. (2007) *Arabidopsis* isochorismate synthase functional in pathogen-induced salicylate biosynthesis exhibits properties consistent with a role in diverse stress responses. *Journal of Biological Chemistry*, 282, 5919–5933.

Thompson, J.D., Higgins, D.G. & Gibson, T.J. (1994) CLUSTAL W: improving the sensitivity of progressive multiple sequence alignment through sequence weighting, position-specific gap penalties and weight matrix choice. *Nucleic Acids Research*, 22, 4673–4680.

Torrens-Spence, M.P., Bobokalonova, A., Carballo, V., Glinkerman, C.M., Pluskal, T., Shen, A. et al. (2019) PBS3 and EPS1 complete salicylic acid biosynthesis from isochorismate in *Arabidopsis*. *Molecular Plant*, 12, 1577–1586.

Valentine, T.A., Randall, E., Wypijewski, K., Chapman, S., Jones, J. & Oparka, K.J. (2007) Delivery of macromolecules to plant parasitic nematodes using a tobacco rattle virus vector. *Plant Biotechnology Journal*, 5, 827–834.

Vlot, A.C., Dempsey, D.A. & Klessig, D.F. (2009) Salicylic acid, a multifaceted hormone to combat disease. *Annual Review of Phytopathology*, 47, 177–206.

Wang, X., Xue, B., Dai, J., Qin, X., Liu, L., Chi, Y. et al. (2018) A novel *Meloidogyne incognita* chorismate mutase effector suppresses plant immunity by manipulating the salicylic acid pathway and functions mainly during the early stages of nematode parasitism. *Plant Pathology*, 67, 1436–1448.

Wen, W., Meinkoth, J.L., Tsien, R.Y. & Taylor, S.S. (1995) Identification of a signal for rapid export of proteins from the nucleus. *Cell*, 82, 463–473.

Wildermuth, M.C., Dewdney, J., Wu, G. & Ausubel, F.M. (2001) Isochorismate synthase is required to synthesize salicylic acid for plant defence. *Nature*, 414, 562–565.

Yang, S., Dai, Y., Chen, Y., Yang, J., Yang, D., Liu, Q. et al. (2019a) A novel G16B09-like effector from *Heterodera avenae* suppresses plant defenses and promotes parasitism. *Frontiers in Plant Science*, 10, 66.

Yang, S., Pan, L., Chen, Y., Yang, D., Liu, Q. & Jian, H. (2019b) *Heterodera avenae* GLAND5 effector interacts with pyruvate dehydrogenase subunit of plant to promote nematode parasitism. *Frontiers in Microbiology*, 10, 1241.

Yu, X., Tang, J., Wang, Q., Ye, W., Tao, K., Duan, S. et al. (2012) The RxLR effector Avh241 from *Phytophthora sojae* requires plasma membrane localization to induce plant cell death. *New Phytologist*, 196, 247–260.

Zhao, J., Li, L., Liu, Q., Liu, P., Li, S., Yang, D. et al. (2019) A MIF-like effector suppresses plant immunity and facilitates nematode parasitism by interacting with plant annexins. *Journal of Experimental Botany*, 70, 5943–5958.

Zhuo, K., Naalden, D., Nowak, S., Xuan Huy, N., Bauters, L. & Gheysen, G. (2019) A *Meloidogyne graminicola* C-type lectin, Mg01965, is secreted into the host apoplast to suppress plant defence and promote parasitism. *Molecular Plant Pathology*, 20, 346–355.

Zimmermann, L., Stephens, A., Nam, S.-Z., Rau, D., Kübler, J., Lozajic, M. et al. (2018) A completely reimplemented MPI bioinformatics toolkit with a new HHpred server at its core. *Journal of Molecular Biology*, 430, 2237–2243.

SUPPORTING INFORMATION

Additional supporting information may be found in the online version of the article at the publisher's website.

How to cite this article: Qin, X., Xue, B., Tian, H., Fang, C., Yu, J., Chen, C. et al. (2021) An unconventionally secreted effector from the root knot nematode *Meloidogyne incognita*, Mi-ISC-1, promotes parasitism by disrupting salicylic acid biosynthesis in host plants. *Molecular Plant Pathology*, 00, 1–14. https://doi.org/10.1111/mpp.13175